

RESEARCH ARTICLE

Theoretical Investigation of Mechanical and Electronic Properties of Hexagonal BaB₂

Cihan Parlak 

Bolu Abant İzzet Baysal University, Faculty of Arts and Sciences, Department of Physics, Bolu/Türkiye

ARTICLE INFO

Article History

Received: 24.10.2023

Accepted: 10.01.2024

First Published: 06.05.2024

Keywords

Ab initio calculations

Elastic properties

Electronic structure

Superconductors



ABSTRACT

A comprehensive investigation of the electronic and mechanical properties in the hexagonal BaB₂ binary system using state of the art first-principles computational techniques is critical for an in-depth understanding of the fundamental properties unique to this binary system. In this context, we derived elastic constants using the metric-tensor formulation, which allowed us to find important mechanical properties such as Bulk Modulus, Shear Modulus, and Vickers's hardness which are fundamental mechanical quantities. Also, this research includes a detailed analysis of the electronic band structures and a study comparison of Fermi surface topologies. The charge density at the Fermi level ($N(E_F)$), which is very important in superconductivity theories, was found to be 1.43 states/eV.uc. Furthermore, we have explored whether there exists a close relationship between these properties and the superconducting behavior of the BaB₂ material. Nevertheless, our calculations unequivocally demonstrate that the information derived from electronic band structures and Fermi surfaces alone is insufficient for a comprehensive explanation of the superconductivity phenomenon observed in such materials.

Please cite this paper as follows:

Parlak, C. (2024). Theoretical investigation of mechanical and electronic properties of hexagonal BaB₂. *Journal of Advanced Applied Sciences*, 3(1), 1-5. <https://doi.org/10.61326/jaasci.v3i1.100>

1. Introduction

The revelation of superconductivity (SC) within MgB₂ (Nagamatsu et al., 2001), a member of the AlB₂-type materials, featuring a critical temperature (T_c) of approximately 39 K, has elicited considerable interest among the scientific community. AlB₂-type structures, recognized for their exceptional attributes encompassing the electron-phonon pairing mechanism, electronic properties, superconductivity, and lattice dynamics, have been a focal point of recent research endeavors.

Although extensive investigations have been conducted on most materials within the AlB₂-type structure, hexagonal BaB₂ has received relatively limited theoretical attention (Alarco et

al., 2015). This scarcity of research may be attributed to the fact that hexagonal BaB₂ has not yet been experimentally synthesized. Nonetheless, this hypothetical material exhibits substantial promise as a high-temperature superconductor (HTS). In light of this, our proposal aims to comprehensively characterize BaB₂ and unveil its mechanic and electronic properties. The ability to calculate the fundamental properties of materials from first-principles calculations has emerged in recent years as an increasingly attractive avenue of research, allowing reliable prediction of a material's properties before experimental verification. This is becoming particularly important in the study of superconductivity (Boeri & Bachelet, 2019; Parlak, 2021).

✉ Correspondence

E-mail address: cihanparlak@gmail.com

This paper is structured as follows: In Part 2, we elucidate our computational methodologies and associated parameters. Part 3.1 delves into an extensive analysis of lattice structure. Section 3.2 provides a concise portrayal of the electronic band structures of the compounds under investigation. Additionally, Section 3.3 furnishes comprehensive data on the elastic properties of these compounds. Our findings culminate in Section 4, offering a succinct recapitulation of our principal results.

2. Materials and Methods

In this investigation, we conducted all computations by employing the ABINIT software (Gonze et al., 2020) in conjunction with the density functional theory (DFT) methodology. The generalized gradient approximation (GGA) was employed for the exchange-correlation functional. To ensure the attainment of convergence, a plane-wave kinetic energy cutoff parameter of 40 Hartree was determined as the optimal choice. K-point sampling for Brillouin zone integrations was achieved using a Monkhorst-Pack mesh with a 16x16x16 grid.

3. Results and Discussion

3.1. Lattice Properties

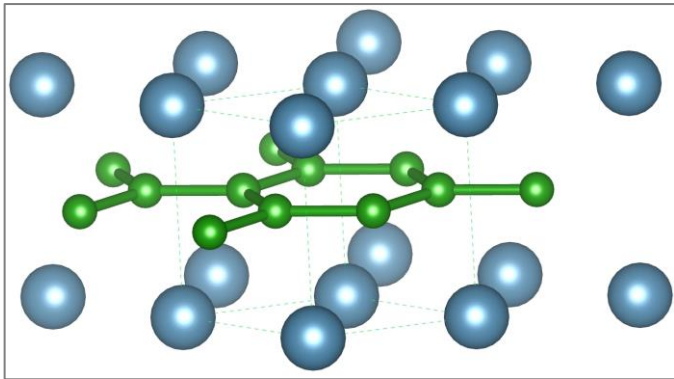


Figure 1. BaB₂ lattice structure, the green color represents B atoms, and the blue color represents Ba atoms.

In the scope of this investigation, we embarked on the optimization of hexagonal di-boride BaB₂ (Figure 1), a representative AlB₂-type material exhibiting the P6/mmm space group (no: 191). Within the well-defined AlB₂-type structural framework, Ba atoms are situated at the 1a (0,0,0) position, while B atoms are precisely situated at the 2d (1/3,2/3,1/2) Wyckoff positions (Parlak, 2020).

In our research, we have successfully acquired optimized lattice parameters for the BaB₂ crystal structure, which are given as $a=3.2842$ Å and $c=4.9551$ Å, our results exhibit a commendable congruence with the relevant data available in the literature (Alarco et al., 2015). If we compare the lattice parameters of BaB₂ with the most basic material of this family,

MgB₂ (with $a=3.086$ Å and $c=3.524$ Å) (Nagamatsu et al., 2001). It is seen that the calculated lattice parameters of BaB₂ are higher than those of MgB₂. This difference will play a role in the difference in basic mechanical and electronic properties.

3.2. Electronic Properties

Possessing knowledge about the electronic band structure of a material affords insight into various physical characteristics of the material. This understanding is particularly significant in the context of superconducting materials, where the electronic structure exerts a direct and profound influence on superconducting properties. Notably, the superconducting transition temperature is acknowledged to exhibit a strong correlation with the electron density at the Fermi level, denoted as $N(E_F)$ (Boeri & Bachelet, 2019).

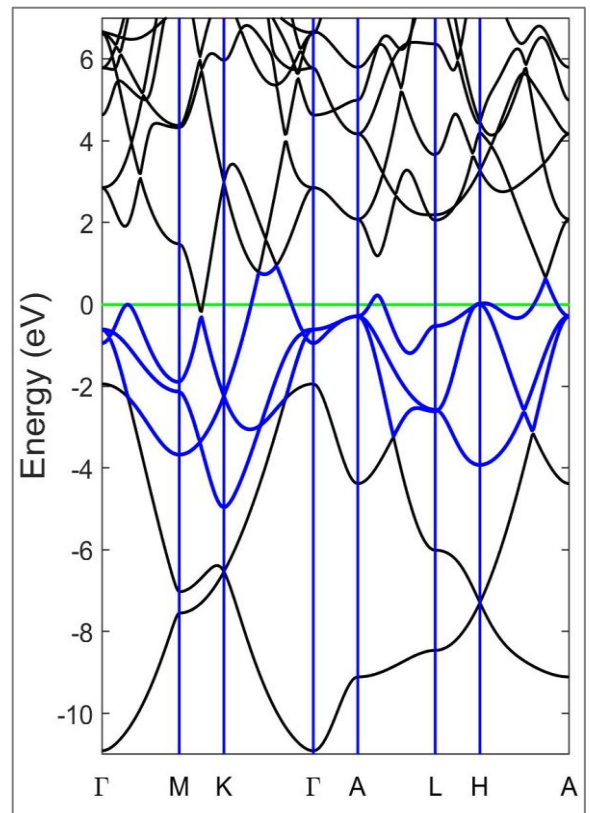


Figure 2. Electronic band structure of BaB₂.

For this reason, in this study, the electronic band structure of the material was calculated in detail (Figure 2). As can be seen from the band structure, the material is completely metallic. One of the most important observations is the conical band structure located between the M-K points of the Brillouin region, very close to the Fermi level. This conical structure has been observed before in some AlB₂ structured materials (Xu et al., 2020) and is directly related to the topological semi-metal nature of the materials.

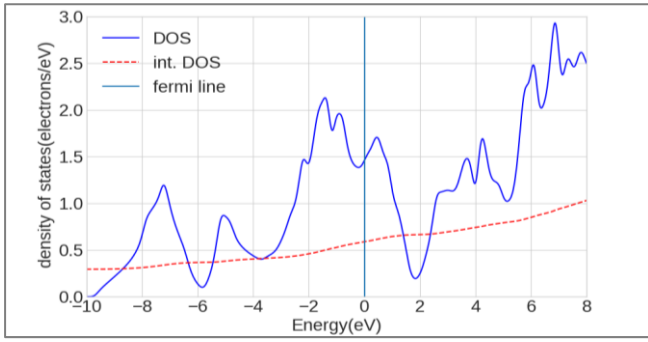


Figure 3. Total electron density of states (DOS).

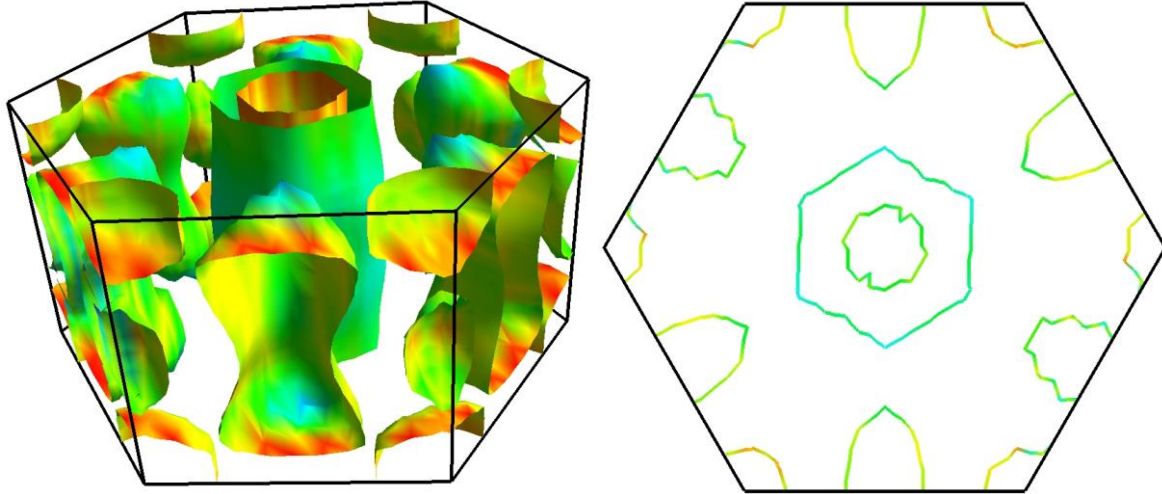


Figure 4. Fermi surface of BaB₂ and 2-D section view at the center of the Brillouin zone.

It would not be wrong to say that BaB₂'s Fermi surfaces consist of three independent surfaces (Figure 4), very similar to MgB₂. Two of them are along Γ -A and are hole-type cylindrical surfaces. The other is an electron-type surface with a 3-dimensional character near the borders of the Brillouin zone. In terms of Fermi surface topography, BaB₂ does not have a very different structure from the general picture seen in other AlB₂ structures and is even very similar to MgB₂.

3.3. Mechanical Properties

The elastic tensor of a material serves as a fundamental tool for gaining deep insights into the material's reactivity under the influence of external forces. This information plays a pivotal role in dissecting the underlying bonding mechanisms and, in turn, enhances our grasp of the multifaceted mechanical and thermal attributes intrinsic to the material (DeJong et al., 2015). In the present investigation, we meticulously calculate the components of the elastic tensor employing the principles of linear response theory, as outlined by Hamann et al. (2005).

These elastic constants are instrumental in elucidating the material's nuanced response to diverse forms of deformation. For instance, C_{11} , C_{12} , and C_{13} specifically characterize the material's behavior under axial deformations, while C_{33} , C_{44} ,

We have given the electron density state of the material in Figure 3. The most striking feature here is the electron state density at the Fermi level is 1.43 States/eV.uc. And it can be said that this value is relatively high compared to MgB₂ (0.69 states/eV.uc (Choi et al., 2009)). From the perspective of superconductivity, although high electron state density at the Fermi level can be expected to cause high T_c, it should not be forgotten that electron-phonon interactions also play an extremely important role in such materials.

and C_{66} are indicative of its response to shear deformations and other anisotropic features.

Furthermore, our findings unequivocally demonstrate that the computed elastic constants conform to the well-established Born criteria for a hexagonal lattice. These criteria, as expounded by Born et al. (1955), encompass conditions such as $C_{11} > 0$, $C_{11} - C_{12} > 0$, and $(C_{11} + C_{12})C_{33} - 2(C_{13})^2 > 0$.

When comparing the elastic constants of BaB₂ ($C_{11}=72.4$, $C_{12}=26.3$, $C_{13}=51.2$, $C_{33}=191.1$, $C_{44}=56.3$, $C_{66}=37.7$ GPa) and MgB₂ ($C_{11}=421$, $C_{12}=64$, $C_{13}=35$, $C_{33}=265$, $C_{44}=70$, $C_{66}=178$ GPa (DeJong et al., 2015)), it's important to consider their mechanical properties and how they differ. These constants help scientists and engineers understand how materials respond to different types of deformation and provide insights into their mechanical behavior. Here's a comparison between the elastic constants of BaB₂ and MgB₂:

- C_{11} (Axial Stiffness): MgB₂ is significantly stiffer in the axial direction, indicating that it is more resistant to compression along this axis.
- C_{12} (Shear Modulus, Shear Stiffness in XY Plane): MgB₂ has a higher shear modulus, suggesting that it is more resistant to shearing forces in the XY plane.

- C_{13} (Shear Modulus, Shear Stiffness in XZ Plane): BaB_2 is stiffer in the XZ plane, indicating its resistance to shearing forces in that direction.
- C_{33} (Axial Stiffness): MgB_2 is stiffer in the axial direction, making it more resistant to compression along this axis.
- C_{44} (Shear Modulus, Shear Stiffness in YZ Plane): MgB_2 has a higher shear modulus in the YZ plane, indicating greater resistance to shearing forces in this direction.
- C_{66} (Shear Modulus, Shear Stiffness in XZ Plane): MgB_2 is significantly stiffer in the XZ plane, making it more resistant to shearing forces in that direction.

In summary of elastic properties, MgB_2 generally has much higher elastic constants compared to BaB_2 , indicating that it is a stiffer and more rigid material. This means that MgB_2 is better suited to withstand higher loads and deformations, especially in axial and shear directions. These differences in elastic constants can have significant implications for the material's mechanical properties and its performance in various applications. Scientists and engineers use these values to design and understand the behavior of materials in a wide range of contexts, from structural engineering to materials science research.

By using the ELATE software (Gaillac et al., 2016), the Voigt–Reuss–Hill approximation (Hill, 1952) can be used for the calculation of some important mechanical constants such as the Bulk (B), Young (E), and Shear (G) moduli. One can see the numerical values in Table 1.

Table 1. Calculated elastic constants (C_{ij}), bulk (B) and shear (G) moduli, Young moduli (E), compressibility (β , in GPa^{-1}), the Pugh's indexes (G/B), Poisson's ratio (ν), Zener anisotropy factor (A), Universal elastic anisotropy index (A^u).

Parameter	Pre. Study	MgB_2^a
B_v	65.91	152.78
G_v	46.81	128.47
B_r	49.36	144.09
G_r	42.52	106.24
B	57.64	148.43
G	44.67	117.35
β	0.0173	0.0067
G/B	0.77	0.79
E	106.49	278.83
ν	0.19	0.18
A	2.44	0.39
A^u	0.84	1.10

^a(DeJong et al., 2015)

Among the fundamental mechanical design parameters, the bulk modulus, defines a material's resistance to compression. In the current study, the Voigt bulk modulus value is

approximately calculated to be 65.91 GPa, while the Reuss bulk modulus value for the BaB_2 material is obtained to be approximately 49.36 GPa. It is clearly seen that both values are much lower than the values given in the table for MgB_2 . These values characterize how effectively the material resists compressive forces.

The Vickers hardness (H_v) parameter of the compound was determined using the microhardness empirical model proposed by Chen and colleagues (Chen et al., 2011). Microhardness is a well-established metric that offers valuable insights into both the elastic and permanent plastic deformations exhibited by the studied compound.

Our findings reveal that at zero pressure, the microhardness parameter are 10.70 GPa (Chen et al., 2011 formulation) and 18.94 GPa (Tian et al., 2012 formulation), indicating a relatively higher resistance to plastic deformation. These observations provide valuable information about the material's response to mechanical stress and have implications for its performance in various applications.

4. Conclusion

In conclusion, our investigation into the electronic and mechanical properties of hexagonal BaB_2 , an AIB_2 -type material with P_6/mmm symmetry, has yielded valuable insights into the fundamental characteristics of this compound. We successfully optimized the lattice parameters. In the realm of electronic properties, our study of the electronic band structure revealed that BaB_2 is a metallic material with a distinctive conical band structure near the Fermi level, reminiscent of other AIB_2 structured materials. The electron density at the Fermi level, $N(E_F)$, was found to be 1.43 States/eV.uc., a relatively high value compared to MgB_2 , indicating potential for superconductivity, though electron-phonon interactions must also be considered. Moreover, the analysis of Fermi surface topography indicated that BaB_2 exhibits three independent surfaces, similar to MgB_2 , further aligning it with the broader AIB_2 family.

In terms of mechanical properties, we have meticulously calculated the elastic constants, providing critical insights into BaB_2 's reactivity to various forms of deformation. Our results affirm that these computed elastic constants adhere to the well-known Born criteria's for a hexagonal lattice. The Voigt bulk modulus, an essential mechanical parameter, was found to be 65.91 GPa, indicating BaB_2 's resistance to compression. Additionally, the microhardness parameter, obtained through empirical models, exhibited a notable resistance to plastic deformation at zero pressure.

In summary, our study advances our understanding of BaB_2 's fundamental properties, offering a comprehensive view of its electronic and mechanical behavior. These findings provide a foundation for further exploration of its potential

applications, including its possible role in superconductivity, and underscore the importance of careful materials characterization and computational modeling in materials science research.

Conflict of Interest

The author has no conflict of interest to declare.

References

- Alarco, J. A., Talbot, P. C., & Mackinnon, I. D. R. (2015). Phonon anomalies predict superconducting T_c for AlB_2 -type structures. *Physical Chemistry Chemical Physics*, 17(38), 25090-25099. <https://doi.org/10.1039/c5cp04402b>
- Boeri, L., & Bachelet, G. B. (2019). Viewpoint: The road to room-temperature conventional superconductivity. *Journal of Physics: Condensed Matter*, 31(23), 234002. <https://doi.org/10.1088/1361-648X/ab0db2>
- Born, M., Huang, K., & Lax, M. (1955). Dynamical theory of crystal lattices. *American Journal of Physics*, 23(7), 474. <https://doi.org/10.1119/1.1934059>
- Chen, X. Q., Niu, H., Li, D., & Li, Y. (2011). Modeling hardness of polycrystalline materials and bulk metallic glasses. *Intermetallics*, 19(9), 1275-1281. <https://doi.org/10.1016/j.intermet.2011.03.026>
- Choi, H. J., Louie, S. G., & Cohen, M. L. (2009). Prediction of superconducting properties of CaB_2 using anisotropic Eliashberg theory. *Physical Review B*, 80(6), 064503. <https://doi.org/10.1103/PhysRevB.80.064503>
- De Jong, M., Chen, W., Angsten, T., Jain, A., Notestine, R., Gamst, A., Sluiter, M., Ande, C. K., van der Zwaag, S., Plata, J. J., Toher, C., Curtarolo, S., Ceder, G., Persson, K. A., & Asta, M. (2015). Charting the complete elastic properties of inorganic crystalline compounds. *Scientific Data*, 2, 150009. <https://doi.org/10.1038/sdata.2015.9>
- Gaillac, R., Pullumbi, P., & Coudert, F. X. (2016). ELATE: An open-source online application for analysis and visualization of elastic tensors. *Journal of Physics: Condensed Matter*, 28(27), 275201. <https://doi.org/10.1088/0953-8984/28/27/275201>
- Gonze, X., Amadon, B., Antonius, G., Arnardi, F., Baguet, L., Beuken, J. M., ... & Zwanziger, J. W. (2020). The ABINIT project: Impact, environment and recent developments. *Computer Physics Communications*, 248, 107042. <https://doi.org/10.1016/j.cpc.2019.107042>
- Hamann, D. R., Wu, X., Rabe, K. M., & Vanderbilt, D. (2005). Metric tensor formulation of strain in density-functional perturbation theory. *Physical Review B*, 71(3), 035117. <https://doi.org/10.1103/PhysRevB.71.035117>
- Hill, R. (1952). The elastic behaviour of a crystalline aggregate. *Proceedings of the Physical Society. Section A*, 65(5), 349. <https://doi.org/10.1088/0370-1298/65/5/307>
- Nagamatsu, J., Nakagawa, N., Muranaka, T., Zenitani, Y., & Akimitsu, J. (2001). Superconductivity at 39 K in magnesium diboride. *Nature*, 410, 63-64. <https://doi.org/10.1038/35065039>
- Parlak, C. (2020). The physical properties of AlB_2 -type structures $CaGa_2$ and $BaGa_2$: An ab-initio study. *Physica B: Condensed Matter*, 576, 411724. <https://doi.org/10.1016/j.physb.2019.411724>
- Parlak, C. (2021). First-principles study of the electronic structure and elastic properties of $SrGa_2$ under pressure. *Materials Today Communications*, 28, 102510. <https://doi.org/10.1016/j.mtcomm.2021.102510>
- Tian, Y., Xu, B., & Zhao, Z. (2012). Microscopic theory of hardness and design of novel superhard crystals. *International Journal of Refractory Metals and Hard Materials*, 33, 93-106. <https://doi.org/10.1016/j.ijrmhm.2012.02.021>
- Xu, S., Bao, C., Guo, P. J., Wang, Y. Y., Yu, Q. H., Sun, L. L., Su, Y., Liu, K., Lu, Z. Y., Zhou, S., & Xia, T. L. (2020). Interlayer quantum transport in Dirac semimetal $BaGa_2$. *Nature Communications*, 11, 2370. <https://doi.org/10.1038/s41467-020-15854-0>